analytical chemistry

pubs.acs.org/ac Article

Doping Nitrogen into Q-Graphene by Plasma Treatment toward Peroxidase Mimics with Enhanced Catalysis

Shuai Li, Xiaoting Zhao, Ruotong Gang, Bingqiang Cao, and Hua Wang*

Cite This: *Anal. Chem.* 2020, 92, 5152−5157 Read Online

ACCESS | Metrics & More | Article Recommendations | Supporting Information

ABSTRACT: A facile and efficient plasma treatment strategy has been applied for the first time to dope heteroatom nitrogen (N) into Q-graphene (QG) under ambient temperature toward a carbon-based green nanozyme. It was discovered that the resulting N doped QG (N-QG) nanozyme can present the greatly enhanced catalysis activity, which is nearly 5-fold higher than that of pristine QG, as comparably revealed by the kinetic studies. Herein, the plasma treatment-assisted N doping could improve the conductivity (hydrophilicity) and create the surface defects of QG so as to promote the electron transferring toward the enhanced catalytic activities of N-QG. Furthermore, the catalase, superoxide dismutase, and oxidase-like catalysis activities of N-QG were explored, indicating the N doping could endow the obtained nanozyme with a high specificity of peroxidase-like catalysis. The application feasibility of the developed N-QG nanozyme was demonstrated subsequently by the catalysis-based colorimetric assays for H_2O_2 in milk samples, with the linear range from 2.00 to 1500 μM. Importantly, such a plasma-assisted heteroatom doping route may open a door toward the large-scale applications for the rational designs of various enzyme mimics with improved catalysis performances.

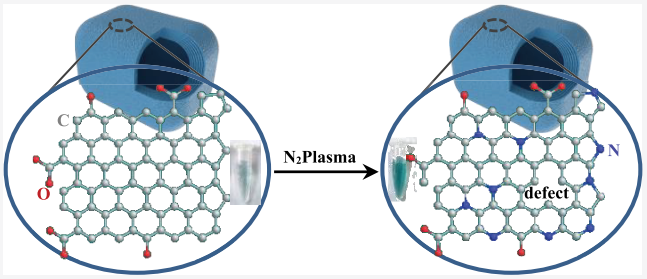

Natural enzymes as the biocatalysts with high catalytic activities and substrate specificity have been widely used in the industrial, environmental, and biomedical catalysis fields.[1−4] However, they may often suffer from some intrinsic shortcomings such as cost ineffectiveness, operational instability, environment-sensitive catalysis activities. Alternatively, many efforts have been devoted to the development of nanozymes due to their high stability, low cost, bulk preparation, and multifunctionalities.[5−7] Since the discovery of Fe_3O_4 nanoparticles with intrinsic peroxidase-like activity in 2007,[8] a large amount of different inorganic nanomaterials have been fabricated and applied, most known as metal oxides, noble metals, and carbon nanomaterials.[9−13] Among them, carbon nanomaterials-based nanozymes have attracted increasing interest in recent years due to their high stability, low cost, and good biocompatibility.[14,15] Q-graphene (QG) as the latest member of graphene family is a nanosphere or polyhedral material consisting of hollow, multiwalled structures with an average particle size of about 80 nm.[16,17] Especially, due to the large surface area, good electrical conductivity, and outstanding thermal and chemical stabilities, QG has been extensively applied in electrochemical sensing fields.[18−20] Yet, the peroxidase-like catalysis activity of QG has not been explored to date. Besides, most of the existing nanozymes including carbon nanomaterials may still encounter moderate catalysis and low specificity, which may challenge their applications on a large scale.

Aiming to improve the catalysis activities in the biological systems, natural enzymes are usually regulated by altering their expressions and compositions at the genetic level or controlling the catalytic environments.[21] Meantime, the catalytic activities of nanozymes have been generally improved by modifying their particle sizes, morphologies, and compositions.[22−25] As the representative example, the chemical doping route of heteroatoms has been widely employed to improve the catalysis activities of nanozymes by increasing their charge-carrier densities and electrical or thermal conductivities.[26] Especially, it is well established that nitrogen (N) is a suitable element to be doped into carbon materials because it can possess the comparable atomic size and five valence electrons available to form strong valence bonds with carbon atoms.[27] For example, Wei and coauthors have chemically doped N into graphene and mesoporous carbon materials showing the increased peroxidase-like activities.[28] Lee's group have described a catalysis-improved peroxidase mimics of N- and B-codoped reduced graphene oxides for sensing applications.[29] However, most of the current chemical doping routes for

Received: December 15, 2019
Accepted: March 9, 2020
Published: March 9, 2020

nanozymes may be challenged by some formidable disadvantages like the complicated operation, harsh conditions (i.e., high-temperature calcinations), and risky impurities introduction. Particularly, the N doping might be even formidable because of its instability under the harsh chemical process.[30]

Plasma as the fourth state of a matter consists of ionic, atomic, molecular, and radical species with an equal number of opposite charges.[31] Nowadays, the plasma treatment technology has been extensively applied as a facile and highly efficient tool for the preparations and/or surface modifications of a variety of functional materials.[32−34] In addition to the high electron temperature and low gas temperature, the plasma treatment is a low energy-consumption process with no chemical waste.[35] Recent years have witnessed the increasing applications of plasma technology in the energy storage or conversion, electrochemical catalysis, and biosensing detection fields.[32,36,37] For example, Lin's group have reported that compared with the pristine graphene, N_2 plasma-treated graphene could present higher electrocatalytic activities for reduction of hydrogen peroxide.[38] Wang et al. utilized the argon plasma-engraving strategy to treat the Co_3O_4 electrocatalyst for oxygen evolution reaction achieving the greatly enhanced current density.[39] However, the plasma treatment technology has hardly been applied for improving the catalysis activities of carbon-based nanozymes to date.

In the present work, a facile and efficient plasma technology has been developed for the first time to dope heteroatom N into QG yielding N-doped QG (N-QG) under ambient temperature. The main fabrication procedure is schematically illustrated in Scheme 1, in which QG was subjected to the N_2 plasma treatment for variable duration so as to tune the N-doping levels for creating surface defect sites on the QG in a highly controllable fashion, in addition to the improved conductivity (hydrophilicity). It was discovered that the resulting N-QG nanozymes could present the greatly enhanced peroxidase-like catalysis, as comparably confirmed by the kinetic studies. Furthermore, the peroxidase-like catalysis specificity of N-QG was systematically studied in detail by comparing with the catalase, superoxide dismutase, and oxidase-like catalysis. Subsequently, a colorimetric strategy was developed using N-QG nanozymes for the detection of H_2O_2 in milk with high sensitivity. To the best of our knowledge, this is the first attempt on the plasma-assisted N doping for carbon nanozymes (i.e., QG) achieving created surface defects and improved conductivity (hydrophilicity) properties toward the enhanced peroxidase-like activity and catalysis specificity.

Scheme 1. Schematic Illustration of the Preparation of N-QG by the N_2 Plasma Treatment for QG

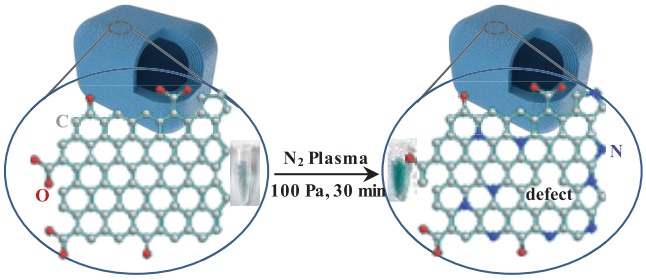

EXPERIMENTAL SECTION

Reagent and Chemicals. Q-graphene (QG) was purchased from Graphene Supermarket Co. Ltd. (Calverton, United States). Catalase, oxidase, superoxide dismutase bovine (SOD), 3,3′,5,5′-tetramethyl benzidine (TMB), hydroethidine (HE), and KO_2 were purchased from Sigma-Aldrich (Shanghai, China). Hydrogen peroxide (30%), anhydrous sodium acetate (NaAc), sodium dihydrogen phosphate dihydrate, and disodium hydrogen phosphate dodecahydrate were purchased from Aladdin (Shanghai, China). All chemical reagents are of analytical grade. Ultrapure water (18.2 MΩ cm, Millipore) was used throughout.

Apparatus and Instruments. PDC-002 plasma cleaning unit (Harrick Plasma) was used for the N_2 plasma treatment of QG. Scanning electron microscopy (SEM) imaging was performed on a Zeiss Sigma 500/VP microscope (Zeiss, Germany). Transmission electron microscopy (TEM) images were collected by a Tecnai G20 microscope (FEI). X-ay photoelectron spectroscopy (XPS) spectra were recorded on a PHI-5000C ESCA system (PerkinElmer). The X-ray diffraction (XRD) investigation was conducted with a Bruker D8 Advance (Bruker, Germany). Raman spectra were recorded by a Thermo Fisher DXR spectrometer (Thermo Fisher). Colorimetric measurements were performed using an Infinite M200 PRO (Tecan, Switzerland).

Preparation of N-Doped QG (N-QG). To prepare N-QG nanozymes, a certain amount of QG was spread on the quartz boat, followed by being placed in the plasma chamber (RF 13.56 MHz, 45 W), which was backfilled with N_2 atmosphere at a pressure of 100 Pa, to be treated for different times of 10, 20, 30, and 40 min. After N_2 plasma treatment, the obtained N-QG products were stored at room temperature and used directly for the catalysis experiments.

Peroxidase-like Activities Measurements. The peroxidase-like catalysis activities of QG and N-QG nanozymes were comparably investigated by catalyzing the chromogenic reactions of TMB and H_2O_2. Briefly, an aliquot of QG or N-QG (1.0 mg/mL, 10 μL) was added into 190 μL of acetate buffer (0.10 M, pH 4.0) containing 0.50 mM TMB and 20 mM H_2O_2. Afterward, the UV−vis absorbance values of the reaction products were monitored at 652 nm using the microplate reader. Besides, the catalytic activities of other kinds of redox enzymes of oxidase, SOD, and catalase were investigated for N-QG in comparison with QG according to the previous report.[40]

Catalase-like Activity Measurements. The catalase-like activities of QG and N-QG were comparably studied by monitoring the catalytic eliminations of H_2O_2 using a UV−visible absorption spectrometer. Typically, an aliquot of QG or N-QG nanozyme (1.0 mg/mL, 10 μL) was added into phosphate buffer (0.10 M, pH 7.0, 190 μL) containing H_2O_2 (0.10 M). After incubation for 20 min, the characteristic absorbance values of reaction solutions at 240 nm were recorded using the microplate reader.

SOD-like Activity Measurements. The SOD-like activities of QG and N-QG were comparably evaluated by monitoring the ability of $^{\bullet}O_2^-$ elimination. Typically, an aliquot of QG or N-QG nanozyme (1.0 mg/mL) was added into acetate buffer (10 mM, pH 4.0) containing $^{\bullet}O_2^-$, which was generated by dissolving 10 μM KO_2 in DMSO solution. After the incubation for 20 min, an aliquot of hydroethidine (0.10 mg/mL) was introduced to react for 20 min. The

https://dx.doi.org/10.1021/acs.analchem.9b05645
Anal. Chem. 2020, 92, 5152−5157

fluorescent intensities of the solutions were recorded with an excitation wavelength of 530 nm.

Kinetic Studies. The steady-state kinetic studies were comparably carried out for QG and N-QG (20 μg/mL), where 0.50 mM TMB or 10 mM H_2O_2 was used alternatively at a fixed concentration of one substrate versus varying concentrations of the other one. All reactions solutions were monitored by measuring the absorbance changes in a kinetic mode at 652 nm. The kinetic parameters were determined using the equation $\nu = V_{max} \times [S]/(K_m + [S])$, where ν is the initial velocity, V_{max} is the maximal velocity, [S] is the concentration of the substrate, and K_m is the Michaelis constant.

Colorimetric Assays for H_2O_2. Typically, an aliquot of H_2O_2 with different concentrations was separately added into acetate buffer (0.10 M, pH 4.0) containing 20 μg/mL N-QG and 0.50 mM TMB. Afterward, the absorbance values of the resulting solutions were recorded at 652 nm by using the microplate reader. Also, the assessments of H_2O_2 levels in milk samples were performed by following the same procedure, of which the samples were prepared using H_2O_2 of different concentrations of spiked fresh milk bought from the local supermarket.

RESULTS AND DISCUSSION

Characterization of N_2 Plasma-Treated QG. The morphological structure of pristine QG was initially examined by scanning electron microscopy (SEM) and transmission electron microscopy (TEM) imaging (Figure S1). One can see from Figure S1A,B that QG consists of hollow and nanosphere or polyhedral morphologies, with an average particle size of about 80 nm. Figure S1C manifests that QG can present a multiwalled structure, more clearly from Figure S1D, showing a total wall thickness of about 6.0 nm. Moreover, the morphological analysis was conducted for the QG after N_2 plasma treatment yielding N-QG (Figure 1). As can be seen from Figure 1A, N-QG could display a clearer profile than QG, although no obvious structure change was observed. Such a phenomenon could also be found from their TEM images (Figure 1B,C), confirming that the N_2 plasma treatment might not cause any structural damage on N-QG so as to expect the well retained electronic properties of QG. Yet, a better dispersion in solution might be preferably achieved for N-QG, due to the N doping possibly endowing the N-QG surfaces with some N-derivatized groups of high polarity, thereby resulting in the increased hydrophilicity, as observed elsewhere for other kinds of N-doped materials.[41] Also, Figure S2 shows the contact angles of the QG surfaces before and after N doping. One can note that after nitrogen plasma treatment for 30 min, the contact angle of QG could decrease from 81.5° to 34.4°, indicating the significantly improved hydrophilicity. Furthermore, the elemental mapping analysis was performed for the obtained N-QG (Figure 1D). One can note that N elements could be homogeneously distributed throughout the N-QG framework, indicating the successful N doping into QG by the plasma treatment. Besides, the X-ray diffraction (XRD) patterns were recorded comparably for QG and N-QG, showing no obvious change in the bulk crystalline phases of QG after the N doping (Figure S3).

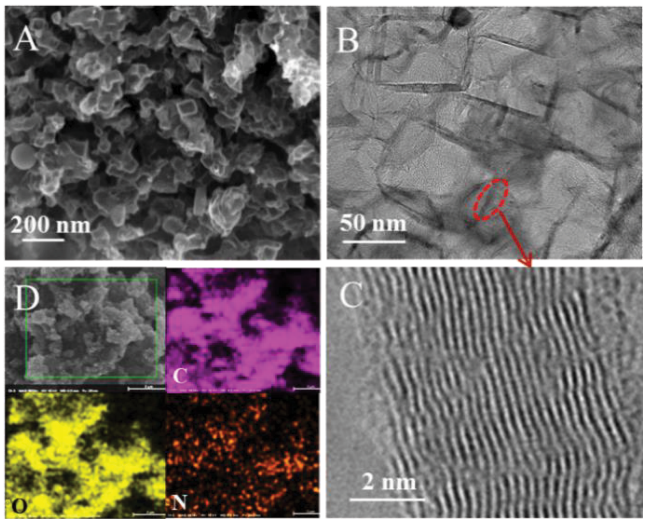

Figure 1. (A) SEM image and (B) TEM images of N-QG with (C) the high-magnitude one and (D) elemental mapping images.

To gain a further insight into the chemical states of N elements doped in N-QG, the X-ray photoelectron spectroscopy (XPS) analysis was performed by taking QG for comparison, with the data shown in Figure 2A. One can see that the N peaks were obtained in the XPS spectra of N-QG at a binding energy (BE) of 398.7 eV for pyridinic-N, 399.9 eV for pyrrolic-N, 401.8 eV for quaternary-N, and 402.8 eV for N-oxides of pyridinic-N, in contrast to that of QG with no apparent N peak. The data indicate that the plasma treatment route could enable the successful incorporation of N into QG toward the formation of N-QG. Moreover, it is well established that the N doping should create the structure defects on the carbon or materials with an increased amount of unsaturated carbon atoms at their edges sites.[42,43] In addition to the easy reaction with oxygen to form oxygen-containing groups, especially, the surface defects might be exposed with more active sites to promote the electron transferring of functional materials leading to the enhanced catalysis.[44] In the present work, the microstructure of N-QG was further identified by using Raman spectroscopy in comparison with QG (Figure 2B). It was found that both of N-QG and QG could present the G band and D band centered at about 1590 and 1360 cm^{-1}, respectively, which may separately arise from the stretching of the C−C sp^2 bond and the sp^3 defect sites. Accordingly, no significant change was found in the positions of the D and G bands. Nevertheless, N-QG could possess a higher intensity ratio of D band to G band (I_D/I_G) than QG, due to the formation of surface defects by the plasma-assisted N doping and etching. Therefore, the significantly enhanced catalysis activities may be expected for N-QG as demonstrated afterward.

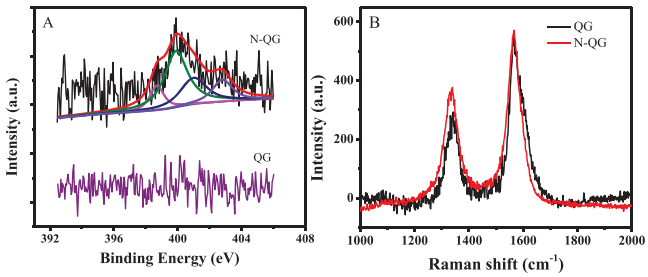

Figure 2. Comparison of (A) core-level high-resolution XPS of N 1s and (B) Raman spectra between QG and N-QG.

https://dx.doi.org/10.1021/acs.analchem.9b05645
Anal. Chem. 2020, 92, 5152−5157

Investigation on the Peroxidase-like Catalysis of N-QG. The peroxidase-like catalytic activities of the prepared N-QG were investigated through catalyzing chromogenic TMB-H_2O_2 reactions by using QG for comparison (Figure 3A). One

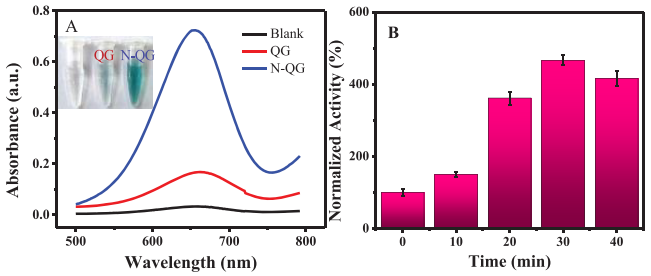

Figure 3. (A) Comparison of peroxidase-like catalysis between QG and N-QG. (B) Peroxidase-like catalysis activities of the obtained N-QG depending on the time of plasma treatment for QG, which were explored by catalyzing TMB-H_2O_2 reactions. Normalized activities (%) = $(A_{N\text{-}QG}/A_{QG}) \times 100\%$, where $A_{N\text{-}QG}$ and A_{QG} refer to the absorbance values of the resulting TMB-H_2O_2 reactions catalyzed by N-QG and QG, respectively.

can see that N-QG could show the much higher catalysis in the oxidation reactions of TMB in the presence of H_2O_2 than QG, as more obviously witnessed by the photographs of the resulting reaction solutions (Figure 3A, inset), confirming that the significantly increased peroxidase-like activities could be obtained by the plasma-aided doping of N into QG. Furthermore, it was experimentally found that the N doping-improved catalytic activities of N-QG could depend on the time of plasma treatment, among which the highest peroxidase-like catalysis of N-QG could be obtained for the N_2 plasma treatment time of 30 min (Figure 3B). Subsequently, the effects of the plasma treatment time on the N amounts doped in QG were explored by the XPS measurements (Figure S4A). It was found that the N amounts could increase to 1.42% as increasing the plasma treatment time up to 30 min, over which the N amounts might be basically unchanged. The results are consistent with those reported elsewhere.[45] Furthermore, the relationship between the N amounts and the normalized catalytic activities of N-QG was obtained (Figure S4B). One can note that the catalytic activities of N-QG could reach the maximum at the N content of 1.42%. Notably, although the N amounts of N-QG might show no substantial change when the plasma treatment over 30 min (i.e., 40 min), the catalytic activities of N-QG might decrease. It implies that the N contents so doped by the plasma treatment may not be the single factor affecting the catalytic activities of N-QG. That is, it may work with other factors, such as the structure defects so created, to facilitate the enhanced catalysis of N-QG. Besides, the catalytic conditions were explored comparably for N-QG and QG, showing the similar catalysis conditions optimized as acetate buffer, pH 4.0, and temperature of 37 °C (Figures S5 and S6).

To further understand the enhanced peroxidase-like activity of N-QG, the steady-state kinetics was investigated in comparison with QG (Figures S7 and S8). Accordingly, as the substrate concentrations increased, both of the catalytic reaction speeds could increase gradually until reaching a plateau, suggesting that their catalytic reactions should obey the Michaelis−Menten kinetics (Figure S7A,C and Figure S8A,C). Further, the apparent Michaelis−Menten parameters were calculated by the typical Lineweaver−Burk double reciprocal curves (Figure S7B,D and Figure S8B,D). The so obtained values of Michaelis constant (K_m) and maximal reaction velocity (V_{max}) were summarized in Table S1. As shown in Table S1, with respect to TMB, the K_m value of N-QG (0.51 mM) was higher than that of QG (0.38 mM), suggesting N-QG has a lower affinity for TMB than QG. However, the K_m value of N-QG (0.069 mM) for H_2O_2 was much lower than that of QG (0.12 mM), indicating that N-QG possesses a higher affinity for H_2O_2 than QG. In addition, the V_{max} values of N-QG for both H_2O_2 and TMB are much higher than those of QG, again confirming that plasma-aided N doping could greatly improve the peroxidase-like catalysis activity of QG. Herein, the dramatically enhanced catalytic activities of N-QG over QG are thought to be attributed to these reasons below. After the N_2 plasma treatment, on the one hand, the hydrophilicity (conductivity) of QG could be enhanced by doped heteroatom N so as to facilitate the resulting N-QG with promoted electron transferring and the easier access of reaction substrates like hydrogen peroxide.[41] On the other hand, the plasma-assisted N doping could create a large number of surface defects on the N-QG surface to accelerate the electron transferring and/or increase reactive sites.[46] What's more, the N introduction might facilitate more radical oxygen species to be produced from the reaction substrates like H_2O_2 and more easily detached from the nanozyme after the catalytic reactions,[28] thus showing the enhanced catalysis of N-QG.

Investigation on the Catalytic Specificity of N-QG Nanozymes. The catalytic activities of other kinds of redox enzymes of oxidase, SOD, and catalase were investigated for N-QG in comparison with QG (Figure S9). Figure S9A illustrates the data of the evaluation of oxidase-like activities of QG and N-QG by monitoring the catalytic oxidation of TMB in the presence of O_2. One can see that both of N-QG and QG could exhibit no significant oxidase-like catalysis, although the N_2 plasma treatment might show a little of improved catalysis. Moreover, the SOD-like catalysis activities of the two nanozymes were evaluated by monitoring the $^{\bullet}O_2^-$elimination ability (Figure S9B). Accordingly, neither N-QG nor QG could eliminate $^{\bullet}O_2^-$ effectively, showing no SOD-like catalysis activity. Besides, the catalase-like catalysis activities of N-QG and QG were comparably explored by monitoring the changing values of characteristic absorbance of H_2O_2 at 240 nm, showing no significant change in the catalase-like catalysis activities (Figure S9C). In particular, a comparison of different kinds of catalytic activities was conducted for N-QG and QG with the data summarized in Figure 4A. One can note that the plasma-assisted N doping could not endow N-QG and QG

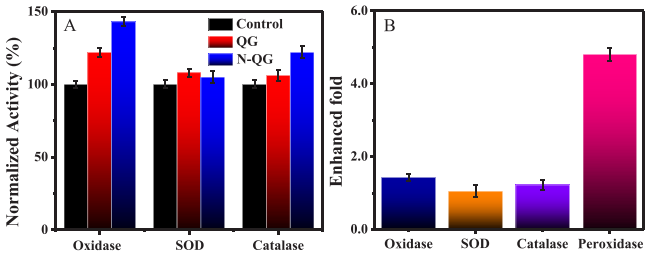

Figure 4. (A) Comparison of oxidase-like, SOD-like, and catalase-like activities between QG and N-QG. (B) Effects of N_2 plasma treatment on the different catalysis activities of N-QG.

https://dx.doi.org/10.1021/acs.analchem.9b05645
Anal. Chem. 2020, 92, 5152−5157

with the improved catalysis activities of other kinds of redox enzymes (oxidase, SOD, and catalase). Yet, a greatly enhanced peroxidase-like catalysis activity could be achieved only for N-QG (Figure 4B). Therefore, the N_2 plasma treatment for QG yielding N-QG could specifically enhance its peroxidase-like catalysis activities by selectively activating the peroxidase substrates like H_2O_2 rather than the oxidase substrate of O_2 or the SOD substrate of $^{\bullet}O_2^-$, as observed elsewhere for other kinds of N-doped carbon materials alternatively by chemical reaction route.[29]

Colorimetric Analysis of H_2O_2. It is well established that the selective detection of H_2O_2 of critical importance can highly depend on the catalysis specificity of enzymes or nanozymes used. Herein, it was demonstrated that the N_2 plasma treatment for QG could not only significantly enhance the peroxidase-like activities but also ensure the high catalytic specificity of N-QG, showing the advantage in the selective detection of H_2O_2.

Under the optimized conditions, the as-prepared N-QG was applied for the catalysis-based colorimetric detection of H_2O_2 in acetate buffer (0.10 M, pH 4.0) (Figure 5A). A linear

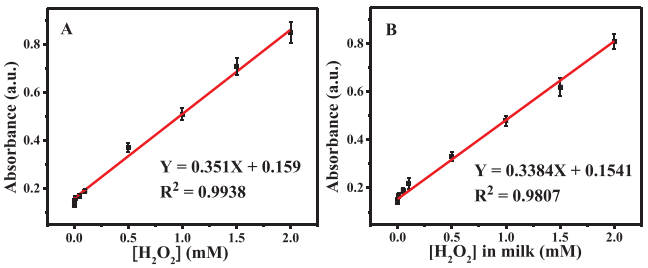

Figure 5. Calibration curves of the relationship between the absorbance responses and different concentrations of H_2O_2 in (A) buffer and (B) in milk samples.

relationship was obtained for the H_2O_2 detection in the linear concentrations ranging from 1.00 to 2000 μM, with the limit of detection (LOD) of about 0.38 μM as estimated by 3σ rule. Furthermore, the feasibility of practical application of the developed colorimetric method was investigated by probing H_2O_2 of different concentrations spiked in milk samples (Figure 5B). The results indicate that H_2O_2 in milk can be detected in the linear the concentrations range of 2.00−1500 μM, with an LOD of about 0.75 μM.

In addition, the analytical performances of the developed colorimetric strategy with N-QG nanozymes for H_2O_2 were compared with those of some current colorimetric methods using other kinds of nanozymes like graphene oxide (GO) and iron oxide (Fe_3O_4), with the comparable results summarized in Table S2.[47−50] It is found that the developed N-QG-based strategy can exhibit better detection performances than the current ones for H_2O_2 in terms of the linear ranges and LODs. Therefore, the developed N-QG-based colorimetric method can allow for the sensitive detection of H_2O_2 in the complicated samples like milk.

CONCLUSIONS

In summary, a facile and efficient plasma treatment strategy was applied for the first time to dope the heteroatom N into QG of carbon-based nanozymes achieving the enhanced peroxidase-like catalysis activities. It was found that the resulting N-QG could possess nearly 5-fold higher catalysis activities than pristine QG, as confirmed by the kinetic studies. A high specificity of peroxidase-like catalysis could also be obtained for N-QG, of which the other kinds of catalysis activities (i.e., oxidase, SOD, and catalase-like catalysis ones) might not be attained by the N doping of QG. The enhanced peroxidase-like catalysis of N-QG is thought to be a result mainly from the N_2 plasma treatment-enhanced hydrophilicity (conductivity) and created surface defects, which might accelerate the electron transferring and/or increase reactive sites for the adjacency of the reaction substrates like H_2O_2. Yet, the detailed mechanism for the N_2 plasma-enhanced catalysis of N-QG should be further explored in the future. Compared with most of the current synthesis routes with harsh conditions (i.e., high temperature and pressure), such a simple and green plasma treatment method can enjoy some superior advantages for the heteroatom doping or modification of functional materials (i.e., simple operation, fast reaction, energy cost-effectiveness, and chemical waste-free product). Besides, H_2O_2 in samples could be quantified by the N-QG-based colorimetric method with the LOD down to about 0.75 μM. More importantly, this plasma treatment-based N doping route may provide a new possibility for the enhancement of catalysis performances of various kinds of nanozymes, thus promising the extensive catalysis applications in the environmental monitoring, food safety, and biomedical analysis fields.

ASSOCIATED CONTENT

Supporting Information

The Supporting Information is available free of charge at https://pubs.acs.org/doi/10.1021/acs.analchem.9b05645.

SEM and TEM images of QG; contact angle measurements; XRD patterns of QG and N-QG; effects of N_2 plasma treatment time on N amounts of N-QG; relationship between N amounts and normalized catalytic activities of N-QG; effects of several buffers on catalytic activities of N-QG; effects of pH and temperature on the peroxidase-like activities of QG and N-QG; steady-state kinetic assays and corresponding double reciprocal plots of QG and N-QG; comparison of kinetic parameters between QG and N-QG; comparison of analytical results for H_2O_2 among different colorimetric methods; and comparison of oxidase-, SOD-, and catalase-like activities between QG and N-QG (PDF)

AUTHOR INFORMATION

Corresponding Author

Hua Wang − *Institute of Medicine and Materials Applied Technologies, College of Chemistry and Chemical Engineering, Qufu Normal University, Qufu City, Shandong Province 273165, P. R. China;* orcid.org/0000-0003-0728-8986; Phone: +86 537 4456306; Email: huawang@qfnu.edu.cn; Fax: +86 537 4456306; http://wang.qfnu.edu.cn

Authors

Shuai Li − *Institute of Medicine and Materials Applied Technologies, College of Chemistry and Chemical Engineering and College of Physics and Engineering, Qufu Normal University, Qufu City, Shandong Province 273165, P. R. China*

Xiaoting Zhao − *Institute of Medicine and Materials Applied Technologies, College of Chemistry and Chemical Engineering,*

Qufu Normal University, Qufu City, Shandong Province 273165, P. R. China

Ruotong Gang − *Institute of Medicine and Materials Applied Technologies, College of Chemistry and Chemical Engineering, Qufu Normal University, Qufu City, Shandong Province 273165, P. R. China*

Bingqiang Cao − *College of Physics and Engineering, Qufu Normal University, Qufu City, Shandong Province 273165, P. R. China;* orcid.org/0000-0002-0866-0076

Complete contact information is available at: https://pubs.acs.org/10.1021/acs.analchem.9b05645

Notes

The authors declare no competing financial interest.

■ ACKNOWLEDGMENTS

This work is supported by the National Natural Science Foundations of China (Grant No. 21675099); Major Basic Research Program of Natural Science Foundation of Shandong Province (Grant ZR2018ZC0129); Special Fund for Post-doctoral Innovation Projects of Shandong Province (Grant 201903045), and Key R&D Plan of Jining City (Grant 2018HMNS001), Shandong, P. R. China.

■ REFERENCES

(1) Liang, M.; Yan, X. *Acc. Chem. Res.* **2019**, *52*, 2190−2200.
(2) Huang, Y.; Ren, J.; Qu, X. *Chem. Rev.* **2019**, *119*, 4357−4412.
(3) Wu, J.; Wang, X.; Wang, Q.; Lou, Z.; Li, S.; Zhu, Y.; Qin, L.; Wei, H. *Chem. Soc. Rev.* **2019**, *48*, 1004−1079.
(4) Wei, H.; Wang, E. *Chem. Soc. Rev.* **2013**, *42*, 6060−6093.
(5) Li, S.; Zhao, X.; Yu, X.; Wan, Y.; Yin, M.; Zhang, W.; Cao, B.; Wang, H. *Anal. Chem.* **2019**, *91*, 14737−14742.
(6) Wu, J.; Li, S.; Wei, H. *Chem. Commun.* **2018**, *54*, 6520−6530.
(7) Xia, W.; Zhang, P.; Fu, W.; Hu, L.; Wang, Y. *Chem. Commun.* **2019**, *55*, 2039−2042.
(8) Gao, L.; Zhuang, J.; Nie, L.; Zhang, J.; Zhang, Y.; Gu, N.; Wang, T.; Feng, J.; Yang, D.; Perrett, S.; Yan, X. *Nat. Nanotechnol.* **2007**, *2*, 577−583.
(9) Deng, H. H.; Luo, B. Y.; He, S. B.; Chen, R. T.; Lin, Z.; Peng, H. P.; Xia, X. H.; Chen, W. *Anal. Chem.* **2019**, *91*, 4039−4046.
(10) Wang, H.; Li, S.; Si, Y.; Sun, Z.; Li, S.; Lin, Y. *J. Mater. Chem. B* **2014**, *2*, 4442−4448.
(11) Li, S.; Zhang, L.; Jiang, Y.; Zhu, S.; Lv, X.; Duan, Z.; Wang, H. *Nanoscale* **2017**, *9*, 16005−16011.
(12) Singh, N.; Savanur, M. A.; Srivastava, S.; D'Silva, P.; Mugesh, G. *Angew. Chem., Int. Ed.* **2017**, *56*, 14267−14271.
(13) Song, Y.; Qu, K.; Zhao, C.; Ren, J.; Qu, X. *Adv. Mater.* **2010**, *22*, 2206−2210.
(14) Sun, H.; Zhou, Y.; Ren, J.; Qu, X. *Angew. Chem., Int. Ed.* **2018**, *57*, 9224−9237.
(15) Wang, H.; Liu, C.; Liu, Z.; Ren, J.; Qu, X. *Small* **2018**, *14*, No. 1703710.
(16) Cai, Y.; Feng, L.; Hua, Y.; Liu, H.; Yin, M.; Lv, X.; Li, S.; Wang, H. *Chem. Commun.* **2018**, *54*, 13595−13598.
(17) Cai, Y.; Jiang, Y.; Feng, L.; Hua, Y.; Liu, H.; Fan, C.; Yin, M.; Li, S.; Lv, X.; Wang, H. *Anal. Chim. Acta* **2019**, *1057*, 88−97.
(18) Luo, Y.; Cai, X.; Li, H.; Lin, Y.; Du, D. *ACS Appl. Mater. Interfaces* **2016**, *8*, 4048−4055.
(19) Hua, Y.; Li, S.; Cai, Y.; Liu, H.; Wan, Y.; Yin, M.; Wang, F.; Wang, H. *Nanoscale* **2019**, *11*, 2126−2130.
(20) Randviir, E. P.; Brownson, D. A. C.; Gómez-Mingot, M.; Kampouris, D. K.; Iniesta, J.; Banks, C. E. *Nanoscale* **2012**, *4*, 6470.
(21) Wilner, O. I.; Weizmann, Y.; Gill, R.; Lioubashevski, O.; Freeman, R.; Willner, I. *Nat. Nanotechnol.* **2009**, *4*, 249−254.
(22) Zhang, Y.; Wang, F.; Liu, C.; Wang, Z.; Kang, L.; Huang, Y.; Dong, K.; Ren, J.; Qu, X. *ACS Nano* **2018**, *12*, 651−661.
(23) Liu, Y.; Xiang, Y.; Zhen, Y.; Guo, R. *Langmuir* **2017**, *33*, 6372−6381.
(24) Cheng, H.; Zhang, L.; He, J.; Guo, W.; Zhou, Z.; Zhang, X.; Nie, S.; Wei, H. *Anal. Chem.* **2016**, *88*, 5489−5497.
(25) Wang, H.; Li, S.; Si, Y.; Zhang, N.; Sun, Z.; Wu, H.; Lin, Y. *Nanoscale* **2014**, *6*, 8107−8116.
(26) Sumpter, B. G.; Meunier, V.; Romo-Herrera, J. M.; Cruz-Silva, E.; Cullen, D. A.; Terrones, H.; Smith, D. J.; Terrones, M. *ACS Nano* **2007**, *1*, 369−375.
(27) Lee, S. U.; Belosludov, R. V.; Mizuseki, H.; Kawazoe, Y. *Small* **2009**, *5*, 1769−1775.
(28) Hu, Y.; Gao, X. J.; Zhu, Y.; Muhammad, F.; Tan, S.; Cao, W.; Lin, S.; Jin, Z.; Gao, X.; Wei, H. *Chem. Mater.* **2018**, *30*, 6431−6439.
(29) Kim, M. S.; Cho, S.; Joo, S. H.; Lee, J.; Kwak, S. K.; Kim, M. I.; Lee, J. *ACS Nano* **2019**, *13*, 4312−4321.
(30) Lou, Z.; Zhao, S.; Wang, Q.; Wei, H. *Anal. Chem.* **2019**, *91*, 15267−15274.
(31) Ke, Z.; Ma, Y.; Zhu, Z.; Zhao, H.; Wang, Q.; Huang, Q. *Appl. Phys. Lett.* **2018**, *112*, No. 013701.
(32) Liu, Y.; Yang, M.; Li, J.; Zhang, W.; Jiang, X. *Anal. Chem.* **2019**, *91*, 6754−6760.
(33) Tao, L.; Duan, X.; Wang, C.; Duan, X.; Wang, S. *Chem. Commun.* **2015**, *51*, 7470−7473.
(34) Gokus, T.; Nair, R. R.; Bonetti, A.; Bohmler, M.; Lombardo, A.; Novoselov, K. S.; Geim, A. K.; Ferrari, A. C.; Hartschuh, A. *ACS Nano* **2009**, *3*, 3963−3968.
(35) Neyts, E. C.; Ostrikov, K. K.; Sunkara, M. K.; Bogaerts, A. *Chem. Rev.* **2015**, *115*, 13408−13446.
(36) Dou, S.; Tao, L.; Wang, R.; El Hankari, S.; Chen, R.; Wang, S. *Adv. Mater.* **2018**, *30*, No. 1705850.
(37) Jiang, Q.; Liu, D.; Zhang, H.; Wang, S. *J. Phys. Chem. C* **2015**, *119*, 28776−28782.
(38) Wang, Y.; Shao, Y.; Matson, D. W.; Li, J.; Lin, Y. *ACS Nano* **2010**, *4*, 1790−1798.
(39) Xu, L.; Jiang, Q.; Xiao, Z.; Li, X.; Huo, J.; Wang, S.; Dai, L. *Angew. Chem., Int. Ed.* **2016**, *55*, 5277−5281.
(40) Yao, J.; Cheng, Y.; Zhou, M.; Zhao, S.; Lin, S.; Wang, X.; Wu, J.; Li, S.; Wei, H. *Chem. Sci.* **2018**, *9*, 2927−2933.
(41) He, Z.; Li, M.; Li, Y.; Wang, L.; Zhu, J.; Meng, W.; Li, C.; Zhou, H.; Dai, L. *Appl. Surf. Sci.* **2019**, *469*, 423−430.
(42) Dou, S.; Tao, L.; Huo, J.; Wang, S.; Dai, L. *Energy Environ. Sci.* **2016**, *9*, 1320−1326.
(43) Shao, Y.; Zhang, S.; Engelhard, M. H.; Li, G.; Shao, G.; Wang, Y.; Liu, J.; Aksay, I. A.; Lin, Y. *J. Mater. Chem.* **2010**, *20*, 7491.
(44) Gao, K.; Wang, B.; Tao, L.; Cunning, B. V.; Zhang, Z.; Wang, S.; Ruoff, R. S.; Qu, L. *Adv. Mater.* **2019**, *31*, No. 1805121.
(45) Rybin, M.; Pereyaslavtsev, A.; Vasilieva, T.; Myasnikov, V.; Sokolov, I.; Pavlova, A.; Obraztsova, E.; Khomich, A.; Ralchenko, V.; Obraztsova, E. *Carbon* **2016**, *96*, 196−202.
(46) Tao, L.; Wang, Q.; Dou, S.; Ma, Z.; Huo, J.; Wang, S.; Dai, L. *Chem. Commun.* **2016**, *52*, 2764−2767.
(47) Wei, H.; Wang, E. *Anal. Chem.* **2008**, *80*, 2250−2254.
(48) Sun, J.; Li, C.; Qi, Y.; Guo, S.; Liang, X. *Sensors* **2016**, *16*, 584.
(49) Jv, Y.; Li, B.; Cao, R. *Chem. Commun.* **2010**, *46*, 8017−8019.
(50) Jin, G.; Ko, E.; Kim, M.; Tran, V.; Son, S.; Geng, Y.; Hur, W.; Seong, G. *Sens. Actuators, B* **2018**, *274*, 201−209.